Published in final edited form as:
Biomaterials. 2011 January ; 32(3): 777–786. doi:10.1016/j.biomaterials.2010.09.044.

A functionalizable reverse thermal gel based on a polyurethane/PEG block copolymer

Daewon Park, **Wei Wu**, and **Yadong Wang***
Department of Bioengineering and the McGowan Institute for Regenerative Medicine, University of Pittsburgh, Pittsburgh, PA 15219

Abstract

Injectable reverse thermal gels have great potentials as biomaterials for tissue engineering and drug delivery. However, most existing gels lack functional groups that can be modified with biomolecules that can guide cell/material interactions. We created an amine-functionalized ABA block copolymer, poly(ethylene glycol)-poly(serinol hexamethylene urethane), or ESHU. This reverse thermal gel consists of a hydrophobic block (B): poly(serinol hexamethylene urethane) and a hydrophilic block (A): poly(ethylene glycol). The polymer was characterized by GPC, FTIR and ^{1}H FTNMR. Rheological study demonstrated that ESHU solution in phosphate-buffered saline initiated phase transition at 32°C and reached maximum elastic modulus at 37°C. The *in vitro* degradation tests performed in PBS and cholesterol esterase solutions revealed that the polymer was hydrolyzable and the presence of cholesterol esterase greatly accelerated the hydrolysis. The *in vitro* cytotoxicity tests carried out using baboon smooth muscle cells demonstrated that ESHU had good cytocompatibility with cell viability indistinguishable from tissue culture treated polystyrene. Subcutaneous implantation in rats revealed well tolerated accurate inflammatory response with moderate ED-1 positive macrophages in the early stages, which largely resolved 4 weeks post-implantation. We functionalized ESHU with a hexapeptide, Ile-Lys-Val-Ala-Val-Ser (IKVAVS), which gelled rapidly at body temperature. We expect this new platform of functionalizable reverse thermal gels to provide versatile biomaterials in tissue engineering and regenerative medicine.

Keywords

Injectable; reverse thermal gel; functionalizable; hexapeptide IKVAVS

1. Introduction

Reverse thermal gels dissolve in water and undergo spontaneous phase transition with increasing temperature and form physical gels at elevated temperatures. They have many uses in biomedicine and biotechnology when their gelling temperature is close to body temperature. The advantage of reverse thermal gel is that they are simple to use and do not require cross-linkers or UV irradiation that are necessary to trigger the gelling of typical

*Corresponding author. Tel.: +1-412-624-7196; Fax: +1-412-383-8788, yaw20@pitt.edu.

Supplementary Data
The sol-gel phase transition window is available as supplementary data in the online version.

hydrogels [1–16]. They retain the advantages of injectable hydrogels in that they can be injected via a thin needle and gel in situ to conform to an irregular shape of the treatment site. Reverse thermal gels only need temperature change to trigger the gelation and shifting the hydrophobicity/hydrophilicity balance can control the gelation temperature [17–21]. However, most existing reverse thermal gels lack functional groups that allow bio-functionalization, which is a powerful way to control cell-biomaterials interaction.

To this end, we designed a reverse thermal gel that has one free primary amine group on every repeating unit. We focused on three factors in the design process. First, what functionality? We chose amine because of its well established conjugation chemistry with biomolecules such as peptides and carbohydrates. Second, which hydrophobic and hydrophilic block? We chose polyurethane as the hydrophobic block because it is widely used in biomedicine and has good biocompatibility [22–27]. We chose PEG as the hydrophilic block because it is non-immunogenic and non-toxic. Third, what the polyurethane monomers should be? Typical polyurethanes are made from a diol and a diisocyanate. We chose serinol as the diol because this serine derivative has two –OH groups and one $–NH_2$ group. The –OH groups can react with the diisocyanate and the $–NH_2$ group can be protected for further biofunctioanlization. Equally important is the biocompatibility of serinol [28,29]. We chose hexamethylene diisocyanate (HDI) because it has been used in many polyurethanes [30–33]. In addition, HDI requires no catalyst, which leads to a cleaner product. Rheological and histological examination demonstrates that ESHU gels rapidly at 37°C and shows good biocompatibility. A bio-functionalized ESHU with IKVAVS peptide also shows quick thermal gelling property.

2. Experimental section

2.1. Materials

N-BOC-serinol and bovine pancreatic cholesterol esterase (CE) (EC 3.1.1.13) were purchased from Sigma-Aldrich (St. Louis, MO, USA). PEG, *N*,*N*′-dicyclohexylcarbodiimide (DCC), and 4-(Dimethyl amino) pyridine (DMAP) were purchased from Alfa Aesar (Ward Hill, MA, USA). Hexamethylene diisocyanate (HDI) was purchased from TCI America (Wellesley Hills, MA, USA). Anhydrous diethyl ether was purchased from Fisher Scientific (Pittsburgh, PA, USA). Anhydrous chloroform, anhydrous dichloromethane, anhydrous N,N-dimethylformamide (DMF), and trifluoroacetic acid (TFA) were purchased from EMD (Gibbstown, NJ, USA). LIVE/DEAD viability/cytotoxicity kit was purchased from Molecular Probes (Carlsbad, CA, USA). Monoclonal antibody (host/isotype: IgG1 kappa) for ED-1 staining was purchased from Millipore (Temecula, CA, USA). The Spectra/Por dialysis membrane (MWCO: 3,500–5,000) was purchased from Spectrum Laboratories (Rancho Domingues, CA, USA). The hex-peptide, I(N-BOC)K(N-BOC)VAVS(tBu)-OH, was synthesized by the peptide synthesis facility at University of Pittsburgh (Pittsburgh, PA, USA).

2.2. Equipment

Fourier transformed infrared (FTIR) spectra were recorded on a Thermo Nicolet iS10 spectrometer equipped with a diamond Smart iTR. ^{1}H FTNMR spectra were recorded on a Bruker Avance 600 NMR. The molecular weight was determined via gel permeation chromatography (GPC) on a Viscotek GPCmax VE2001 system equipped with a Viscotek I-MBMMW-3078 column and a Viscotek 270 dual detector (differential refractive index and right angle light scattering) using THF as the eluent. Polyethylene glycol (American Polymer Standard) was used for calibration. Rheological measurements were performed on a thermostatted oscillating rheometer (PHYSICA MCR301, Anton Paar) equipped with a 5 cm steel cone (1 degree). 1.0 ml of the polymer solution was used for the measurements.

The data was collected at an angular frequency of 1 rad/s with 0.5% strain. All *in vitro* cell morphologies were examined on a Nikon ECLIPSE TE 200 equipped with digital camera (RT Color, 1× HRD 100-NIK, Diagnostic Instruments). All histological examinations including image acquisition were performed on a Nikon ECLIPSE T*i* equipped with a Qimaging RETIGA-SRV digital camera. The LIVE/DEAD assay was recorded on a Microplate Reader using Gen5 software (SYNERGY Mx, BioTek).

2.3. Synthesis of ESHU

2.3.1. Synthesis of polyurethane block (Step 1)—N-BOC-serinol (0.5 g, 2.62 mmol) was placed in a 25 ml round bottom flask and melted at 90°C under a nitrogen atmosphere. HDI (0.44 g, 2.62 mmol) was added slowly and the polymerization was performed for 150 min to form the urethane bonds (Fig. 1). More HDI (0.88 g, 5.24 mmol) was added and the reaction mixture was stirred for 6 h to synthesize the polyurethane middle block (**intermediate I**). After cooling down to ambient temperature, the mixture was dissolved in 2 ml anhydrous chloroform and poured into excess anhydrous diethyl ether to precipitate out the polymer. The purification process was carried out twice and the precipitates were washed in 100 ml of anhydrous diethyl ether overnight to remove unreacted HDI. **Intermediate I** was obtained after drying at 45°C under vacuum (yield: 97%).

2.3.2. Coupling of polyurethane block and PEG (Step 2)—As synthesized **intermediate I** (1 g) and PEG (3 g, M_w: 550) were placed in a 25 ml round bottom flask and the reaction was performed at 90°C for 6 h under a nitrogen atmosphere. After cooling down, the mixture was dissolved in 2 ml of anhydrous chloroform, precipitated into excess anhydrous diethyl ether twice, and washed in 100 ml of anhydrous diethyl ether. A transparent ESHU was obtained after drying at 45°C overnight under vacuum (yield: 95%, M_w: 3,955, M_w/M_n: 1.66).

Additionally we synthesized large molecular weight of ESHU. We followed the same procedure as described above with a little modification. N-BOC-serinol (0.5 g, 2.62 mmol) was dissolved in 1 ml anhydrous DMF in a 25 ml round bottom flask at 90°C under a nitrogen atmosphere. HDI (0.44 g, 2.62 mmol) was added slowly and the polymerization was performed. After 48 h, HDI (22 mg, 0.131 mmol) was added to facilitate the reaction. The polymerization was performed for 7 days. More HDI (0.88 g, 5.24 mmol) was added and the reaction mixture was stirred for 12 h. After cooling down to ambient temperature, the mixture was precipitated in excess anhydrous diethyl ether. The polymer was dissolved again in 2 ml anhydrous chloroform and poured into excess anhydrous diethyl ether to precipitate out the polymer. The purification process was carried out twice and the precipitates were washed in 100 ml of anhydrous diethyl ether overnight to remove unreacted HDI. The intermediate was obtained after drying at 45°C under vacuum (yield: 98%). As synthesized intermediate (1 g) and PEG (3 g, M_w: 550) were dissolved in 2 ml anhydrous DMF in a 25 ml round bottom flask and the reaction was performed at 90°C for 12 h under a nitrogen atmosphere. After cooling down, the mixture was precipitated into excess anhydrous diethyl ether. After drying, the polymer was further purified with dialysis membrane in water at room temperature for 3 days. The dialyzed solution was freeze-dried and a transparent ESHU was obtained (yield: 97%, M_w: 17,600, M_w/M_n: 2.1).

2.4. *In vitro* degradation

The degradation of ESHU was performed in pure PBS and CE solution as previously described [33,34]. For enzymatic degradation, ESHU was dissolved in 5 ml PBS to form a 5 wt % solution and incubated with 400 units/ml CE at 37°C on a stirrer at 60 rpm. One unit of CE was defined as the concentration of enzyme required to produce 1.0 nmol of cholesterol from cholesteryl oleate per minute. A 0.2 ml of fresh CE solution (2000 units/

ml) was added to the polymer solutions every three days to maintain CE activity. At each time point, 1 ml sample was taken from each solution, lyophilized, dissolved in THF, and filtered (0.2 μm) for GPC analysis. The degradation in PBS was studied in the same way as in CE except no enzyme was used.

2.5. Cytotoxicity tests on ESHU

Non-immortalized baboon smooth muscle cells (P14) were isolated from a 4-year-old male *Papio cyncephalus* and used for *in vitro* cytotoxicity tests. Cells were cultured in MCDB 131 medium with 10% fetal bovine serum (FBS), 1% L-glutamine and 20 μg/ml gentamycin. The cells were incubated in a humidified atmosphere with 5% CO_2 at 37°C. The medium was refreshed every three days until the cells reached 95% confluence. The cells were harvested from the petri dish by incubation in 1 ml of trypsin solution (0.25%) for 20 min, neutralizing with 5 ml of serum-supplemented medium, centrifugation and removal of supernatant. The cell pellets were resuspended in serum-supplemented medium at a concentration of 4×10^5 cells/ml and used immediately for cytotoxicity test.

The cytotoxicity was evaluated according to ISO 10993-5 guideline [35]. Briefly, 400 mg of the polymer was extracted using 1 ml of serum-supplemented MCDB 131 culture medium for 24 h at 37°C. After incubation for 24 h, 0.5 ml of each extract and 100 μl of baboon smooth muscle cell suspension (4×10^4 cells) were placed in 24-well plates. Fresh serum-supplemented medium was used as control. After 24 h of incubation, the cell morphology was examined on a fluorescent microscope. The cell viability was determined by LIVE/DEAD viability/cytotoxicity kit containing calcein AM and ethidium homodimer-1 (EthD-1). After 24 h of incubation, the cell culture medium was removed and cells were rinsed with sterile PBS solution. A 100 μl of LIVE/DEAD assay reagent that consists of 2 μmol calcein AM and 4 μmol EthD-1 was added and incubated for 30 min at room temperature. After staining, the cells were examined on a fluorescence microscope to determine viability. The cell viability was further quantified using a Microplate Reader. The excitation/emission wavelengths were 485/515nm and 525/590nm for calcein AM and EthD-1, respectively.

2.6. *In vivo* biocompatibility

Male Sprague-Dawley rats weighing 225–275 g were used in a preliminary investigation of the in vivo biocompatibility of ESHU. All animal experiments were performed under a protocol approved by the Institutional Animal Care and Use Committees (IACUC) at the University of Pittsburgh. The solution of 60% (wt/v) ESHU was chosen for *in vivo* injection because it was the highest concentration in water which represents the largest dose of the polymer and would represent the most severe host response. Prior to and during polymer injection, the rats were anesthetized by isoflurane (2–3%) inhalation. Under sterile conditions, 0.5 ml of ESHU solution was injected subcutaneously at the lower right and lower left back of each rat. The solutions gelled quickly and round humps can be palpated under the skin. The animals were sacrificed and injection site explanted after 3, 14, 28 days. The tissues were fixed in 10% formalin for histological analysis, or frozen in OCT for ED1 immunohistochemical analysis. For haematoxylin and eosin (H&E) staining and Masson's trichrome staining (MTS), fixed specimens were serially dehydrated in a graded series of ethanol washes and embedded in paraffin. Eight micron thick sections were cut along the longitudinal axis of each implant and stained according to standard protocols for H&E and MTS staining. An immunohistochemical procedure was used to stain ED1, a marker of newly recruited macrophages. The frozen specimens were cut into 8-μm thick sections, fixed in acetone for 10 min, and then air dried. Nonspecific binding was blocked by a 30-min incubation in normal goat serum (5% v/v, 0.1% Triton X100, 0.1M PBS, pH 7.4). The slide was then incubated in mouse anti-rat ED1 primary antibody (1:100, 0.1% Triton 100X,

0.1M PBS) (Abcam, Cambridge, MA) for 40 mins at 37°C. After three PBS washes, the slides were again blocked in normal horse serum and exposed to goat anti-mouse Cy3 secondary antibody (1:400, 0.1% Triton 100X, 0.1M PBS) (Abcam, Cambridge, MA) for 30 min at room temperature, and followed by three PBS washes. ED1 stained sections were analyzed for the density of newly recruited macrophages. Nine 200× magnification images were obtained for each specimen. The number of ED1+ cells in a given area was quantified using Nikon NIS-Elements software.

2.7. Functionalization of ESHU with IKVAVS

2.7.1. De-protection of ESHU (NH_2-ESHU)—As synthesized ESHU (100 mg) was dissolved in 10 ml chloroform in a 50 ml round bottom flask. TFA (10 ml) was added and BOC de-protection was performed for 1 h at room temperature. After removing TFA and chloroform by rotary evaporation, the polymer was purified using dialysis in water at room temperature for 2 days. The dialyzed solution was freeze-dried and a pale yellowish solid (NH_2-ESHU) was obtained (yield: 96%).

2.7.2. Synthesis of IKVAVS conjugated ESHU (IKVAVS-ESHU)—I(BOC)K(BOC)VAVS(tBu)-OH (83 mg, 0.095 mmol) was dissolved in 23 ml anhydrous DMF in a 50 ml round bottom flask. DCC (21.6 mg, 0.105 mmol) solution in 1 ml anhydrous DMF was added slowly at 0°C. NH_2-ESHU (50 mg, 0.19 mmol NH_2) solution in 1 ml anhydrous DMF was added with a catalytic amount of DMAP, which was stirred for 24 h at room temperature under a nitrogen atmosphere. The cyclohexylurea was filtered off. After removing 90% DMF using rotary evaporator, it was poured into excess diethyl ether to precipitate out I(BOC)K(BOC)VAVS(tBu)-ESHU. After drying, BOC was removed in 20 ml chloroform/TFA (50/50, v/v) mixture for 1 h at room temperature. After removing TFA and chloroform using rotary evaporator, the polymer was purified by dialysis in water at room temperature for 2 days. The dialyzed solution was freeze-dried and a pale yellowish solid, IKVAVS-ESHU, was obtained (yield: 86.3%).

3. Results and Discussion

3.1. Structural Characterization

We monitored the progress of the polymerization reaction using FTIR. The most prominent changes were observed on isocyanate groups and ether linkage. The isocyanate groups of **intermediate I** (Fig. 2A) at 2250 cm^{-1} disappeared after PEGylation, whereas the ether linkage of PEG block in ESHU (Fig. 2B) appeared at 1100 cm^{-1} indicating PEGylation occurred to both isocyanate end groups of **intermediate I**. The strong peak at 1680 cm^{-1} was assigned to carbonyl groups of amide bonds. Moreover, other characteristic peaks such as amide N-H and urethane C-O-C were observed at 1520 and 1250 cm^{-1}, respectively.

To further examine the chemical structures of ESHU, we performed ^1H FTNMR analysis (Fig. 3). The methylene protons in PEG (a) and N-BOC-serinol (d) were confirmed at 3.65 and 4.0–4.2 ppm, respectively. The methylene protons adjacent to nitrogen in HDI unit (e) were observed at 3.17 ppm. The protons bound to nitrogen in HDI and N-BOC-serinol (b,c) were confirmed at 4.85–5.25 ppm. The signal at 1.42 ppm was assigned to methyl protons in the BOC groups.

The hydrophobic:hydrophilic ratio of reverse thermal gels is an important factor to determine thermal behaviors such as gelling rate and phase transition temperature. To estimate the hydrophobic:hydrophilic ratio, we measured molecular weights (M_w) of ESHU. The M_w of ESHU was 3,955 with relatively narrow PDI (1.66). We designated the value, calculated by the M_w of PEG subtracted from M_w of ESHU, as the M_w of hydrophobic

block. The ratio was calculated by the comparison of M_w of PEG and hydrophobic block. Thus, the ratio of hydrophobic:hydrophilic was 2.6 which was in the range (1.2 – 6) as reported previously [21,36–38].

3.2. Sol-gel phase transition

Reverse thermal gels undergo sol-gel phase transitions caused by rapid changes in solubility upon heating or cooling. They are fluidic at low temperatures and gel at elevated temperatures. Further heating beyond the gelation temperature can result in phase separation. To use reverse thermal gels as injectable biomaterials, it should gel at body temperature. We investigated the phase transition phenomenon of ESHU rheologically by measuring elastic modulus upon temperature sweep and time sweep (Fig. 4). No significant changes in elastic modulus were observed below 30°C indicating it remained fluidic (Fig. 4A). A sharp increase in elastic modulus was observed between 30–39°C corresponding to the sol to gel phase transition. Further heating over 39°C led to a decrease in elastic modulus corresponding to phase separation. Although the gelling and phase separation temperature depended on the polymer concentrations, all the polymer solutions remained gel at body temperature (see supplementary data Fig. S1). To estimate how fast ESHU can gel in the human body, we measured the elastic modulus at 37°C (Fig. 4B). Regardless of concentration, the rapid increase in elastic modulus completed within 3 min suggesting that ESHU solution can form a gel quickly upon injection. These observations indicate that ESHU possesses appropriate thermal properties for biomedical applications.

3.3. *In vitro* degradation

Degradation rate is an important parameter of biomaterials, especially those intended for applications in tissue engineering and drug delivery. To determine the degradability of ESHU, we measured the changes of M_w in PBS and CE solution at 37°C. The degradation rate was expressed as the ratio of the M_w upon degradation and that of the new polymer (Fig. 5). No significant changes of M_w were observed in 14 days in PBS and approximately 1.9% decrease was observed at day 45. The presence of CE greatly accelerated the degradation, which reached 6.6, 12.0 and 20.2% in 7, 14 and 45 days respectively. There are many evidences of *in vitro* degradation of polyurethanes by enzymes such as chymotrypsin [39,40] and CE [34,41,42]. Polyurethanes can also be degraded by oxidation. An *in vivo* oxidative environment can be formed by immune system via macrophages and foreign body giant cells. Several researches have revealed that polyurethanes were degraded by oxidation mimicking an *in vivo* biodegradation mechanism of immune system [40,43–46]. Thus the biodegradation rate of ESHU is expected to be faster *in vivo*.

3.4. *In vitro* cytotoxicity

The *in vitro* cytotoxicity of ESHU was examined according to ISO 10993-5 guideline on extraction methods to evaluate the toxicity of biomaterials. The morphologies of cells exposed to the extracts (Fig. 6B) resembled that on the control (Fig. 6A) and most cells are viable after exposure to the extracts as indicated by green fluorescence micrographs captured in the live/dead assay (Fig. 6D). These images are consistent with the high percentage of live cells observed in live/dead assay (Fig. 6E). All numbers were calculated by comparing the fluorescence of live and dead cells collected by the microplate reader. The percentage of live cells was statistically the same as the control based on a two-tailed Student's *t*-test. We did not perform viability test with diluted solutions because the original extracts showed good cytocompatibility.

3.5. *In vivo* biocompatibility

In order to investigate host response of ESHU, *in vivo* biocompatibility test was performed. We examined the highest possible concentration of ESHU to test the most severe host response. All the animals survived throughout the study with no malignant infection and abscess at the injection sites. Tissues adjacent to the polymer showed native histological structure with regular muscle alignment and cell morphology at 3 days (Fig. 7A, D and G). H&E staining revealed the presence of significant inflammatory infiltrates around the polymer. MTS staining showed a loose collagen layer (blue) surrounding the polymer and appeared to be newly formed and immature. Two weeks post-injection (Fig. 7B, E and H), the tissues surrounding polymer showed regular cell morphology and alignment. The amount of inflammatory infiltrate decreased significantly and MTS staining showed collagen depositions around the polymer appeared to be more mature. Generally, the tissues surrounding the polymer showed characters of fibrous tissues, and host cells infiltrated into the polymer and began to remodel the gel. Four weeks after injection (Fig. 7C, F and I), the inflammation was largely resolved with tissue architecture surrounding the polymer mostly returned to normal. The polymers and the host tissue appeared to be well integrated. Cellular remodeling occurred in most part of the gel. Tissues within the gel contained smaller amount of collagen and had less organized structures than the surrounding tissues.

ED1 staining was used to estimate macrophage activities triggered by the injection of the gel. At 3 days (Fig. 8A), a large number of newly recruited (ED1-positive) macrophages aggregated around the polymers and presented red-stained band around the implant, which indicated an acute inflammatory reaction. We attributed this to a non-specific inflammatory reaction because it was widely observed in many implanted biomaterials [47]. Two weeks post-injetion (Fig. 8B), the density of ED1-positive cells decreased slightly. However, there was no difference statistically. Four weeks after injection (Fig. 8C), the density of ED1-positive cells significantly decreased and the band of newly-recruited macrophages disappeared indicating the infiltration of macrophages into the gel and the cellular remodeling of the material accompanied by mild inflammatory reactions. To quantify ED1+ macrophages, 5 images were chosen randomly around tissue-ESHU interface and quantified using Nikon NIS-Elements software. The sequential and significant decrease in the number of macrophages per square millimeter from 1589 at 3 days to 1329 at 14 days and 194 at 28 days indicating a mild inflammation that was mostly resolved by 4 weeks (Fig. 8D). Thus, ESHU showed biocompatibility in SC implantation even at the highest dose.

3.6. Functionalization of ESHU with IKVAVS

Typical components of injectable reverse thermal gels are poly(L-lactic acid) [48,49], poly[(lactic acid)-co-(glycolic acid)] [18,50], poly(ε-caprolactone) [51,52] and poly(N-isopropylacrylamide) [53,54]. These polymers show good biocompatibility and sol-gel phase transitions around body temperature. There is a significant emphasis on functionalized injectable gels for biomedical applications. Recent reports include tertiary amines [55–57], a RGD conjugated poly(organophosphazene) [58], and a dopamine conjugated hyaluronic acid [59]. We created a serine-based reverse thermal gel by simple chemistry without catalyst. The polymer is easy to purify and contains a primary amine group in each repeating unit that leads to versatile bio-functionalization. To verify the ability of bio-functionalization using the ESHU platform, we investigated a reaction between ESHU and IKVAVS. IKVAV is a laminin epitope that is known as a promotor of cell adhesion and neurite outgrowth [60–63]. To reserve the bioactivity of IKVAV, we needed a spacer amino acid that directly reacts with the primary amine of NH_2-ESHU. We chose **Ser** because IKVAVS is the natural sequence in laminin. To our knowledge, this is the first report of an IKVAVS-containing thermal gel.

We monitored the incorporation of IKVAVS using FTIR. The most prominent change was observed on carbonyl peaks between 1600–1700 cm^{-1}. The NH_2-ESHU showed one carbonyl peak from amide bonds of ESHU backbone at 1680 cm^{-1} (Fig. 9A). However, IKVAVS-ESHU showed two carbonyl groups at 1680 and 1630 cm^{-1}. The peak at 1680 cm^{-1} was same as the one in NH_2-ESHU. The peak at 1630 cm^{-1} was assigned to carbonyl groups from peptide bonds in IKVAVS-ESHU which was a strong evidence that IKVAVS was incorporated well (Fig. 9B). Other characteristic peaks such as ether linkage of PEG block, amide N-H, and urethane C-O-C were observed at 1100, 1520, and 1250 cm^{-1}, respectively.

We further examined the chemical structure of IKVAVS-ESHU using ^1H FTNMR analysis (Fig. 10). The inset displaying the spectrum of NH_2-ESHU showed no BOC groups at 1.42 ppm indicating a clean de-protection. The most prominent difference between NH_2-ESHU and IKVAVS-ESHU was observed in the range of 0.8–2.2 ppm (dotted area). The methyl protons in **Ile** (a), **Ala** (c), **Val** (e) were observed at 0.93, 1.62, and 1.17 ppm, respectively. The methylene protons in **Lys** (b) were observed at 1.75 and 1.87 ppm. The hydroxyl proton in **Ser** (d) appeared at 2.04 ppm. The degree of substitution of IKVAVS was 41.3% as calculated by the ratio of the methylene proton in **Lys** and the methylene protons “f” in the polymer backbone (same designation as in Fig 3).

In order to investigate the potential as an injectable biomaterial, the elastic modulus of IKVAVS-ESHU was studied rheologically as described previously. In our previous works (data not shown), the solution of IKVAVS-ESHUs synthesized from low M_w of ESHU exhibited no thermal gelling properties regardless of concentrations. We deduced that the IKVAVS-ESHUs from low M_w were too hydrophilic to gel. Indeed an increase in the M_W of the hydrophobic block of ESHU led to successful thermal gelation of IKVAVS-ESHU. The elastic modulus of this polymer solution increased with increasing temperature and formed gel at body temperature (Fig. 11). A dramatic increase in elastic modulus was observed between 28–36°C. The polymer completely gelled at 37°C (Fig. 11A) with no significant changes in elastic modulus until phase separation at 43°C. The measurement of the change of elastic modulus at 37°C mimicked the injection into a human body, which showed the polymer solution gelled completely in less than a minute (Fig. 11B). These demonstrated that the IKVAVS-functionalized ESHU was an injectable thermal gel.

We successfully functionalized ESHU with IKVAVS through the primary amine groups on the polymer. The conjugation of IKVAVS led to changes of physicochemical properties. We monitored the structural changes by FTIR. The overall spectra of ESHU (Fig. 2B), NH_2-ESHU (Fig. 9A), and IKVAVS-ESHU (Fig. 9B) were the same except the appearance of two carbonyl peaks in the IKVAVS-ESHU spectrum. We observed single carbonyl peak in both ESHU and NH_2-ESHU at 1680 cm^{-1} originated from the urethane bonds. In contrast, IKVAVS-ESHU exhibited an additional carbonyl stretch at 1630 cm^{-1} corresponding to amide groups of the peptide bonds in IKVAVS. We further monitored structural changes by ^1H FTNMR. The general proton signals of ESHU (Fig. 3) and NH_2-ESHU (Fig. 10 inset) were the same except that the methyl protons in ESHU at 1.42 ppm disappeared in the spectra of NH_2-ESHU indicating the removal of BOC protective groups. On the other hand, IKVAVS-ESHU displayed a vastly different ^1H FTNMR spectrum (Fig. 10) at 0.8–2.2 ppm: New proton signals appeared at a, b, c, d, and e that corresponded to **Ile**, **Lys, Ala**, **Ser,** and **Val** respectively. The appearance of an additional strong amide stretch in IR and the correlated additional proton signals in NMR are indicative of functionalization with IKVAVS. The functionalization also led to the change of elastic property upon heating. The dramatic increase in elastic modulus of ESHU was observed at 30–39°C, and it decreased right after reaching maximum elastic modulus (Fig. 4A). Whereas the dramatic increase in elastic modulus of IKVAVS-ESHU was observed at 28–36°C and maintained its gel state

until 43°C (Fig. 11A), much longer than ESHU gel. The rate of sol to gel phase transition at body temperature was also changed. IKVAVS-ESHU formed a complete gel in 40 sec (Fig. 11B) which was much faster than ESHU (3 min, Fig. 4B). These observations correlated well with the hydrophobic nature of IKVAVS, and the functionalization resulted in faster phase transition and a more stable gel.

4. Conclusions

We designed and characterized an amine-functionalized biodegradable reverse thermal gel based on serinol. The amine functional group was further functionalized with IKVAVS, and resultant IKVAVS-ESHU showed good thermal gelling property. We are currently investigating the effect of IKVAVS-ESHU on the regeneration of central nerve system. We believe this platform of functionalizable reverse thermal gels could lead to significant innovations in tissue engineering and regenerative medicine.

Supplementary Material

Refer to Web version on PubMed Central for supplementary material.

Acknowledgments

The authors would like to acknowledge financial support from the National Institutes of Health (R21EB008565). The authors thank Drs. Keewon Lee and Jin Gao for assistance with cell culture. The authors are grateful to Dr. Sachin Velankar for helpful discussions on rheological study and Dr. Rui Liang for assistance with fluorescence microscopy.

References

1. Hiratani H, Fujiwara A, Tamiya Y, Mizutani Y, Alvarez-Lorenzo C. Ocular release of timolol from molecularly imprinted soft contact lenses. Biomaterials 2005;26:1293–8. [PubMed: 15475059]
2. Park H, Temenoff JS, Tabata Y, Caplan AI, Mikos AG. Injectable biodegradable hydrogel composites for rabbit marrow mesenchymal stem cell and growth factor delivery for cartilage tissue engineering. Biomaterials 2007;28:3217–27. [PubMed: 17445882]
3. Taguchi T, Xu LM, Kobayashi H, Taniguchi A, Kataoka K, Tanaka J. Encapsulation of chondrocytes in injectable alkali-treated collagen gels prepared using poly(ethylene glycol)-based 4-armed star polymer. Biomaterials 2005;26:1247–52. [PubMed: 15475054]
4. Justin G, Guiseppi-Elie A. Characterization of electroconductive blends of poly(HEMA-co-PEGMA-co-HMMA-co-SPMA) and poly(Py-co-PyBA). Biomacromolecules 2009;10:2539–49. [PubMed: 19705837]
5. Yeom J, Bhang SH, Kim BS, Seo MS, Hwang EJ, Cho IH, et al. Effect of cross-linking reagents for hyaluronic acid hydrogel dermal fillers on tissue augmentation and regeneration. Bioconjug Chem 21:240–7. [PubMed: 20078098]
6. Yeo Y, Geng WL, Ito T, Kohane DS, Burdick JA, Radisic M. Photocrosslinkable hydrogel for myocyte cell culture and injection. J Biomed Mater Res Part B 2007;81B:312–22.
7. Miller JS, Shen CJ, Legant WR, Baranski JD, Blakely BL, Chen CS. Bioactive hydrogels made from step-growth derived PEG-peptide macromers. Biomaterials 31:3736–43. [PubMed: 20138664]
8. Akdemir ZS, Akcakaya H, Kahraman MV, Ceyhan T, Kayaman-Apohan N, Gungor A. Photopolymerized injectable RGD-modified fumarated poly(ethylene glycol) diglycidyl ether hydrogels for cell growth. Macromol Biosci 2008;8:852–62. [PubMed: 18504803]
9. Lin CC, Metters AT, Anseth KS. Functional PEG-peptide hydrogels to modulate local inflammation induced by the pro-inflammatory cytokine TNF alpha. Biomaterials 2009;30:4907–14. [PubMed: 19560813]
10. D'Erricot G, De Lellis M, Mangiapia G, Tedeschi A, Ortona O, Fusco S, et al. Structural and mechanical properties of UV-photo-cross-linked poly(N-vinyl-2-pyrrolidone) hydrogels. Biomacromolecules 2008;9:231–40. [PubMed: 18163572]

11. Obara K, Ishihara M, Ozeki Y, Ishizuka T, Hayashi T, Nakamura S, et al. Controlled release of paclitaxel from photocrosslinked chitosan hydrogels and its subsequent effect on subcutaneous tumor growth in mice. J Control Release 2005;110:79–89. [PubMed: 16289419]
12. Mann BK, Gobin AS, Tsai AT, Schmedlen RH, West JL. Smooth muscle cell growth in photopolymerized hydrogels with cell adhesive and proteolytically degradable domains: synthetic ECM analogs for tissue engineering. Biomaterials 2001;22:3045–51. [PubMed: 11575479]
13. Mann BK, Schmedlen RH, West JL. Tethered-TGF-beta increases extracellular matrix production of vascular smooth muscle cells. Biomaterials 2001;22:439–44. [PubMed: 11214754]
14. Sahoo S, Chung C, Khetan S, Burdick JA. Hydrolytically degradable hyaluronic acid hydrogels with controlled temporal structures. Biomacromolecules 2008;9:1088–92. [PubMed: 18324776]
15. Burdick JA, Ward M, Liang E, Young MJ, Langer R. Stimulation of neurite outgrowth by neurotrophins delivered from degradable hydrogels. Biomaterials 2006;27:452–9. [PubMed: 16115674]
16. Fairbanks BD, Schwartz MP, Bowman CN, Anseth KS. Photoinitiated polymerization of PEG-diacrylate with lithium phenyl-2,4,6-trimethylbenzoylphosphinate: polymerization rate and cytocompatibility. Biomaterials 2009;30:6702–7. [PubMed: 19783300]
17. Tang Y, Singh J. Biodegradable and biocompatible thermosensitive polymer based injectable implant for controlled release of protein. Int J Pharm 2009;365:34–43. [PubMed: 18786623]
18. Lee DS, Shim MS, Kim SW, Lee H, Park I, Chang TY. Novel thermoreversible gelation of biodegradable PLGA-block-PEO-block-PLGA triblock copolymers in aqueous solution. Macromol Rap Commun 2001;22:587–92.
19. Oh HJ, Joo MK, Sohn YS, Jeong B. Secondary structure effect of polypeptide on reverse thermal gelation and degradation of L/DL-poly(alanine)-poloxamer-L/DL-poly(alanine) copolymers. Macromolecules 2008;41:8204–9.
20. Ogura M, Tokuda H, Imabayashi SI, Watanabe M. Preparation and solution behavior of a thermoresponsive diblock copolymer of poly(ethyl glycidyl ether) and poly(ethylene oxide). Langmuir 2007;23:9429–34. [PubMed: 17676779]
21. Kim SY, Kim HJ, Lee KE, Han SS, Sohn YS, Jeong B. Reverse thermal gelling PEG-PTMC diblock copolymer aqueous solution. Macromolecules 2007;40:5519–25.
22. Smith JC, Davies MC, Melia CD, Denyer SP, Derrick MR. Uptake of drugs by catheters: The influence of the drug molecule on sorption by polyurethane catheters. Biomaterials 1996;17:1469–72. [PubMed: 8853116]
23. Woodhouse KA, Klement P, Chen V, Gorbet MB, Keeley FW, Stahl R, et al. Investigation of recombinant human elastin polypeptides as non-thrombogenic coatings. Biomaterials 2004;25:4543–53. [PubMed: 15120499]
24. Park JH, Lee KB, Kwon IC, Bae YH. PDMS-based polyurethanes with MPEG grafts: Mechanical properties, bacterial repellency, and release behavior of rifampicin. J Biomater Sci-Polym Ed 2001;12:629–45. [PubMed: 11556741]
25. Khorasani MT, Shorgashti S. Fabrication of microporous thermoplastic polyurethane for use as small-diameter vascular graft material. I. Phase-inversion method. J Biomed Mater Res Part B 2006;76B:41–8.
26. Matsuda H, Miyazaki M, Oka Y, Nakao A, Choda Y, Kokumai Y, et al. A polyurethane vascular access graft and a hybrid polytetrafluoroethylene graft as an arteriovenous fistula for hemodialysis: Comparison with an expanded polytetrafluoroethylene graft. Artif Organs 2003;27:722–7. [PubMed: 12911347]
27. Alferiev I, Stachelek SJ, Lu ZB, Fu AL, Sellaro TL, Connolly JM, et al. Prevention of polyurethane valve cusp calcification with covalently attached bisphosphonate diethylamino moieties. J Biomed Mater Res Part A 2003;66A:385–95.
28. Tomlinson R, Klee M, Garrett S, Heller J, Duncan R, Brocchini S. Pendent chain functionalized polyacetals that display pH-dependent degradation: A platform for the development of novel polymer therapeutics. Macromolecules 2002;35:473–80.
29. Rickerby J, Prabhakar R, Patel A, Knowles J, Brocchini S. A biomedical library of serinol-derived polyesters. J Control Release 2005;101:21–34. [PubMed: 15588891]

30. Sarkar D, Yailg JC, Sen Gupta A, Lopina ST. Synthesis and characterization of L-tyrosine based polyurethanes for biomaterial applications. J Biomed Mater Res Part A 2009;90A:263–71.
31. Gorna K, Gogolewski S. Preparation, degradation, and calcification of biodegradable polyurethane foams for bone graft substitutes. J Biomed Mater Res Part A 2003;67A:813–27.
32. Eglin D, Grad S, Gogolewski S, Alini M. Farsenol-modified biodegradable polyurethanes for cartilage tissue engineering. J Biomed Mater Res Part A 2010;92A:393–408.
33. Zhang CH, Zhao KJ, Hu TY, Cui XF, Brown N, Boland T. Loading dependent swelling and release properties of novel biodegradable, elastic and environmental stimuli-sensitive polyurethanes. J Control Release 2008;131:128–36. [PubMed: 18703098]
34. Christenson EM, Patel S, Anderson JM, Hiltner A. Enzymatic degradation of poly(ether urethane) and poly(carbonate urethane) by cholesterol esterase. Biomaterials 2006;27:3920–6. [PubMed: 16600363]
35. ISO document 10993. Biological evaluation of medical devices. Part 5: Tests for in vitro cytotoxicity. 1999
36. Kim HK, Shim WS, Kim SE, Lee KH, Kang E, Kim JH, et al. Injectable in situ-forming pH/thermo-sensitive hydrogel for bone tissue engineering. Tissue Eng Part A 2009;15:923–33. [PubMed: 19061427]
37. Jeong B, Kim SW, Bae YH. Thermosensitive sol-gel reversible hydrogels. Adv Drug Deliv Rev 2002;54:37–51. [PubMed: 11755705]
38. He CL, Kim SW, Lee DS. In situ gelling stimuli-sensitive block copolymer hydrogels for drug delivery. J Control Release 2008;127:189–207. [PubMed: 18321604]
39. Rockwood DN, Woodhouse KA, Fromstein JD, Chase DB, Rabolt JF. Characterization of biodegradable polyurethane microfibers for tissue engineering. J Biomater Sci-Polym Ed 2007;18:743–58. [PubMed: 17623555]
40. Sarkar D, Lopina ST. Oxidative and enzymatic degradations of L-tyrosine based polyurethanes. Polym Degrad Stabil 2007;92:1994–2004.
41. Tang YW, Labow RS, Santerre JP. Enzyme-induced biodegradation of polycarbonate polyurethanes: Dependence on hard-segment concentration. J Biomed Mater Res 2001;56:516–28. [PubMed: 11400129]
42. Tang YW, Labow RS, Santerre JP. Enzyme induced biodegradation of polycarbonate-polyurethanes: dose dependence effect of cholesterol esterase. Biomaterials 2003;24:2003–11. [PubMed: 12628819]
43. Christenson EM, Anderson JM, Hiltner A. Oxidative mechanisms of poly(carbonate urethane) and poly(ether urethane) biodegradation: In vivo and in vitro correlations. J Biomed Mater Res Part A 2004;70A:245–55.
44. McBane JE, Santerre JP, Labow RS. The interaction between hydrolytic and oxidative pathways in macrophage-mediated polyurethane degradation. J Biomed Mater Res Part A 2007;82A:984–94.
45. Schubert MA, Wiggins MJ, Schaefer MP, Hiltner A, Anderson JM. Oxidative biodegradation mechanisms of biaxially strained poly(etherurethane urea) elastomers. J Biomed Mater Res 1995;29:337–47. [PubMed: 7542244]
46. Schubert MA, Wiggins MJ, Anderson JM, Hiltner A. Role of oxygen in biodegradation of poly(etherurethane urea) elastomers. J Biomed Mater Res 1997;34:519–30. [PubMed: 9054535]
47. Sundback CA, Shyu JY, Wang YD, Faquin WC, Langer RS, Vacanti JP, et al. Biocompatibility analysis of poly(glycerol sebacate) as a nerve guide material. Biomaterials 2005;26:5454–64. [PubMed: 15860202]
48. Jeong B, Bae YH, Lee DS, Kim SW. Biodegradable block copolymers as injectable drug-delivery systems. Nature 1997;388:860–2. [PubMed: 9278046]
49. Choi SW, Choi SY, Jeong B, Kim SW, Lee DS. Thermoreversible gelation of poly(ethylene oxide) biodegradable polyester block copolymers. II. J Polym Sci Part A-Polym Chem 1999;37:2207–18.
50. Hou QP, Chau DYS, Pratoomsoot C, Tighe PJ, Dua HS, Shakesheff KM, et al. In situ gelling hydrogels incorporating microparticles as drug delivery carriers for regenerative medicine. J Pharm Sci 2008;97:3972–80. [PubMed: 18240277]

51. Gou ML, Li XY, Dai M, Gong CY, Wang XH, Xie Y, et al. A novel injectable local hydrophobic drug delivery system: Biodegradable nanoparticles in thermo-sensitive hydrogel. Int J Pharm 2008;359:228–33. [PubMed: 18448286]
52. Jo S, Kim J, Kim SW. Reverse thermal gelation of aliphatically modified biodegradable triblock copolymers. Macromol Biosci 2006;6:923–8. [PubMed: 17099865]
53. Hacker MC, Klouda L, Ma BB, Kretlow JD, Mikos AG. Synthesis and characterization of injectable, thermally and chemically gelable, amphiphilic poly(N-isopropylacrylamide)-based macromers. Biomacromolecules 2008;9:1558–70. [PubMed: 18481893]
54. Chen JP, Cheng TH. Preparation and evaluation of thermo-reversible copolymer hydrogels containing chitosan and hyaluronic acid as injectable cell carriers. Polymer 2009;50:107–16.
55. Nguyen MK, Park DK, Lee DS. Injectable poly(amidoamine)-poly(ethylene glycol)-poly(amidoamine) triblock copolymer hydrogel with dual sensitivities: pH and temperature. Biomacromolecules 2009;10:728–31. [PubMed: 19296656]
56. Dayananda K, He C, Park DK, Park TG, Lee DS. pH- and temperature-sensitive multiblock copolymer hydrogels composed of poly(ethylene glycol) and poly(amino urethane). Polymer 2008;49:4968–73.
57. Huynh DP, Nguyen MK, Pi BS, Kim MS, Chae SY, Kang CL, et al. Functionalized injectable hydrogels for controlled insulin delivery. Biomaterials 2008;29:2527–34. [PubMed: 18329707]
58. Chun C, Lim HJ, Hong KY, Park KH, Song SC. The use of injectable, thermosensitive poly(organophosphazene)-RGD conjugates for the enhancement of mesenchymal stem cell osteogenic differentiation. Biomaterials 2009;30:6295–308. [PubMed: 19712969]
59. Lee Y, Chung HJ, Yeo S, Ahn CH, Lee H, Messersmith PB, et al. Thermo-sensitive, injectable, and tissue adhesive sol-gel transition hyaluronic acid/pluronic composite hydrogels prepared from bio-inspired catechol-thiol reaction. Soft Matter 6:977–83.
60. Silva GA, Czeisler C, Niece KL, Beniash E, Harrington DA, Kessler JA, et al. Selective differentiation of neural progenitor cells by high-epitope density nanofibers. Science 2004;303:1352–5. [PubMed: 14739465]
61. Tysseling-Mattiace VM, Sahni V, Niece KL, Birch D, Czeisler C, Fehlings MG, et al. Self-assembling nanofibers inhibit glial scar formation and promote axon elongation after spinal cord injury. J Neurosci 2008;28:3814–23. [PubMed: 18385339]
62. Heller DA, Garga V, Kelleher KJ, Lee TC, Mahbubani S, Sigworth LA, et al. Patterned networks of mouse hippocampal neurons on peptide-coated gold surfaces. Biomaterials 2005;26:883–9. [PubMed: 15353199]
63. Santiago LY, Nowak RW, Rubin JP, Marra KG. Peptide-surface modification of poly(caprolactone) with laminin-derived sequences for adipose-derived stem cell applications. Biomaterials 2006;27:2962–9. [PubMed: 16445976]

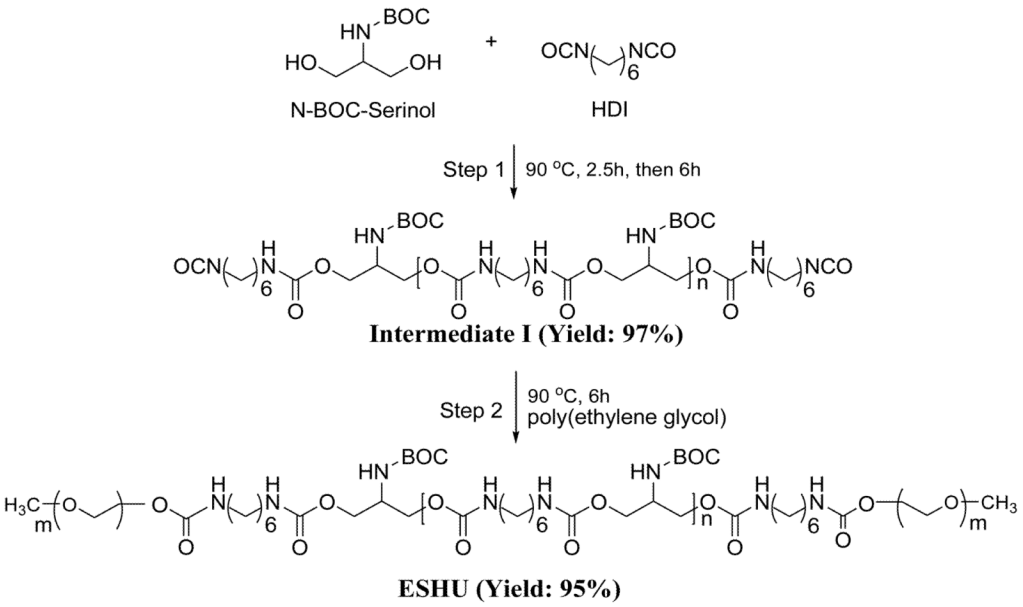

Fig. 1.

Synthesis of ESHU. Step 1: synthesis of polyurethane **intermediate I**. Step 2: PEGylation of **intermediate I** to obtain ESHU. BOC: *tert*-Butyl carbamate protecting group; HDI: hexamethylene diisocyanate.

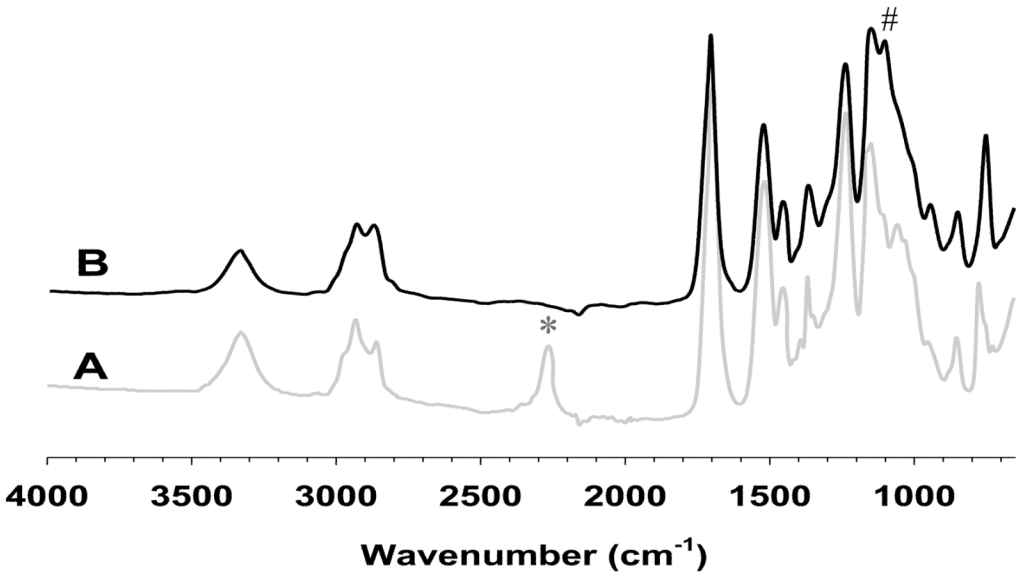

Fig. 2.

FTIR spectra of (A) **intermediate I** and (B) ESHU. The reactive isocyanate groups of **intermediate I** at 2250 cm^{-1} (*) completely disappeared while ether linkage corresponding to PEG in ESHU at 1100cm^{-1} (#) appeared after the PEGylation.

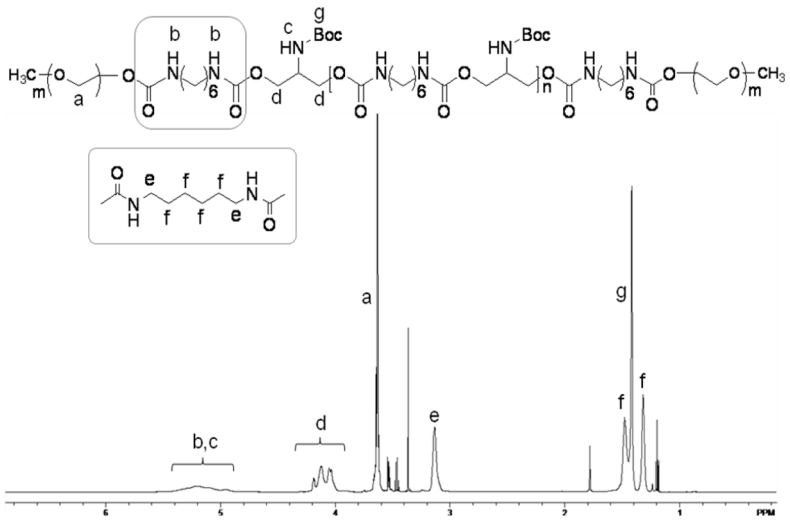

Fig. 3.

^{1}H FTNMR spectra of ESHU in $CDCl_3$. The presence of **a**, **e** and **g** protons indicate the presence of PEG, polyurethane and BOC-protected amine groups in ESHU.

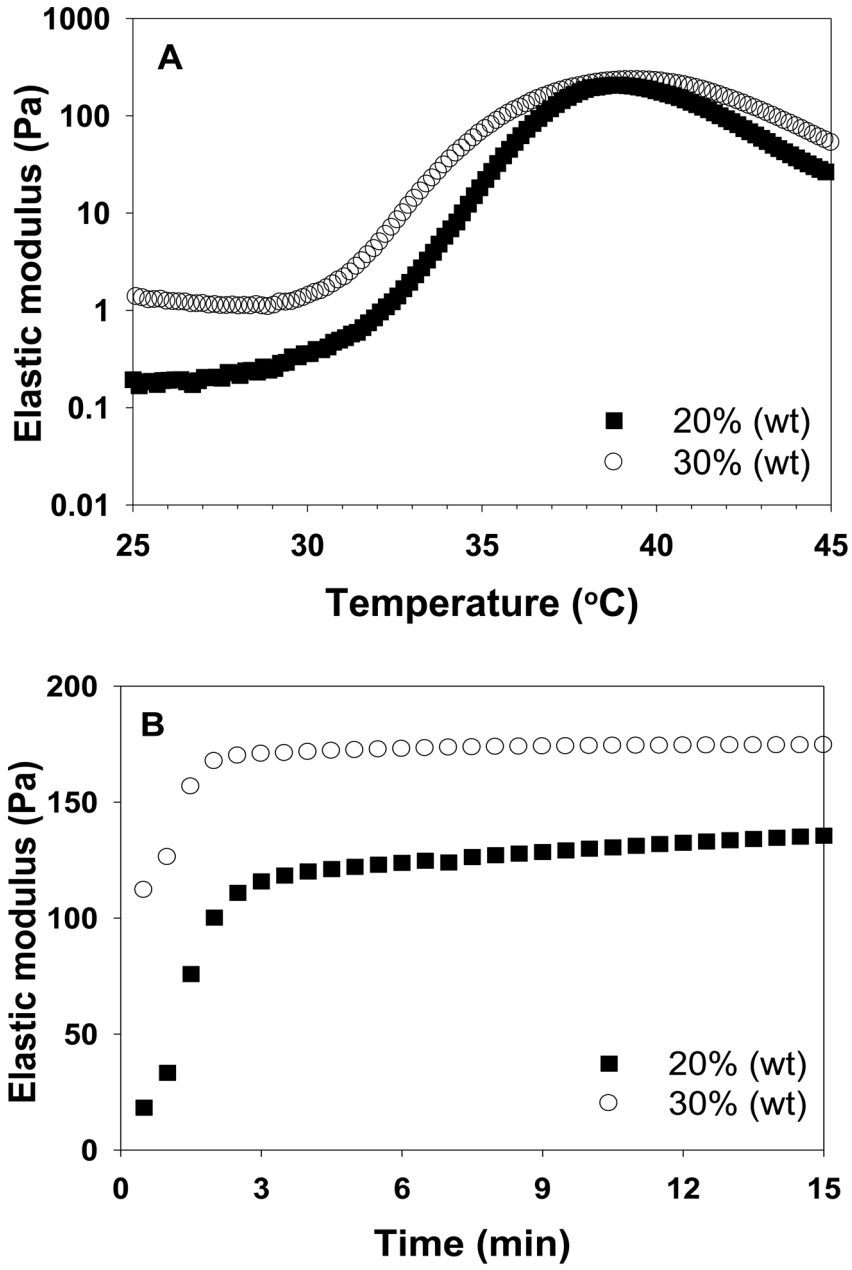

Fig. 4.

The elastic modulus of ESHU. (A) Temperature sweep was recorded in the temperature range of 25–45°C (0.5°C/min) at concentrations of 20 and 30% (wt). (B) Time sweep was recorded at 37°C at concentrations of 20 and 30% (wt) for 15 min. The rapid change of elastic modulus upon heating indicated a sol to gel phase transition. The decrease in elastic modulus caused by further heating beyond gelation indicated phase separation. The polymer solution formed a gel in 3 min at 37°C.

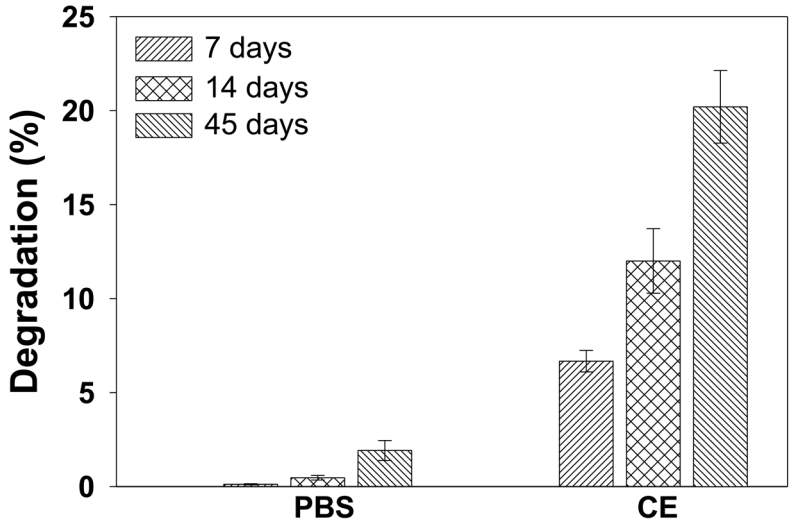

Fig. 5.

In vitro degradation of ESHU in PBS and CE solution. The degradation of ESHU was much faster in the presence of CE. Data are presented as means ± S.D (n=3).

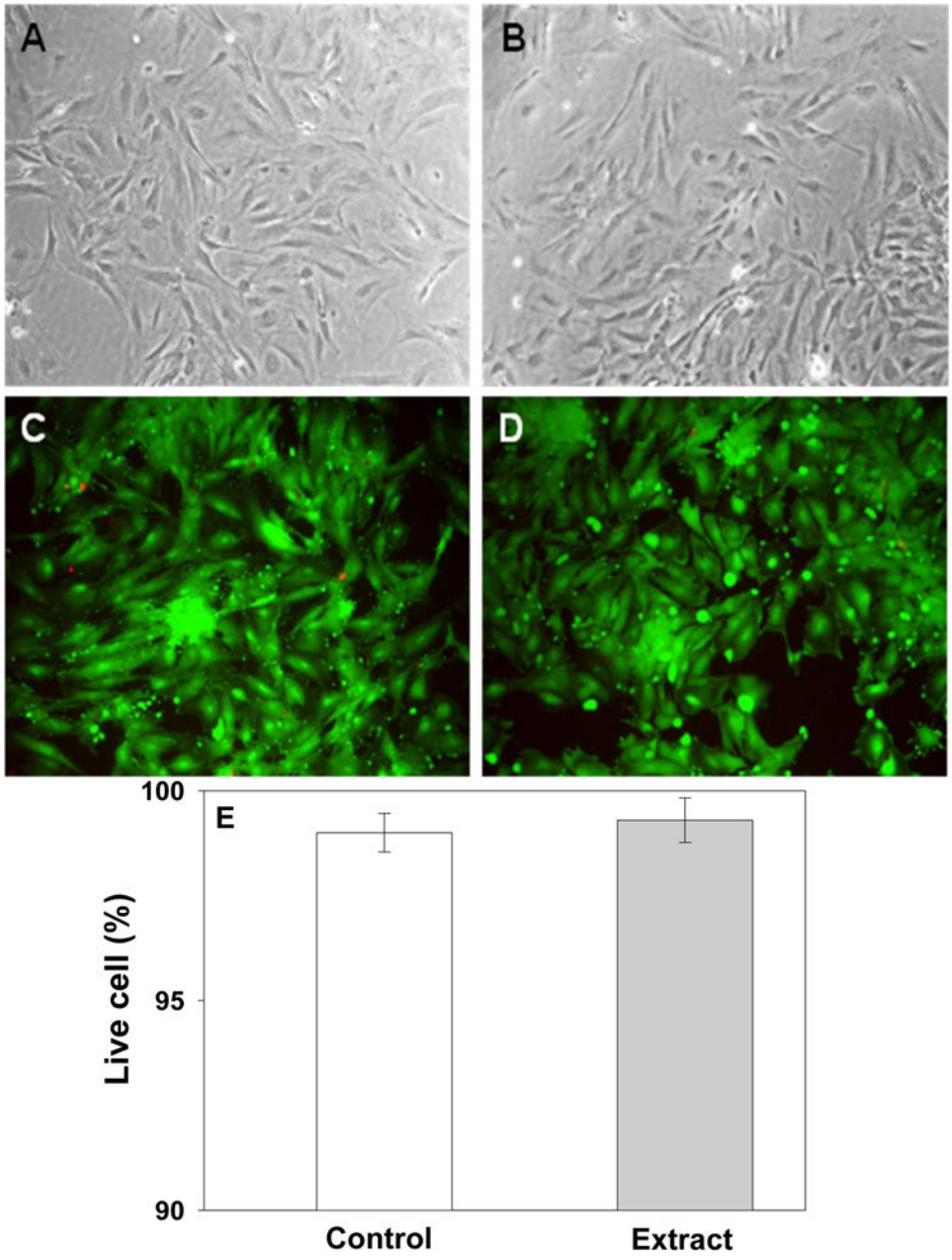

Fig. 6.

In vitro cytotoxicity of ESHU toward baboon smooth muscle cells by MCDB extracts for 24 h at 37°C. Phase contrast of cell morphologies of control (A) and extract (B). No differences were observed between control and extract. Fluorescence images of cells of (C) control and (D) extract which stained with LIVE/DEAD assay reagent. All images produced mostly green fluorescence with a few red one. All images were taken with 200× magnification. (E) The percentage of live cells by LIVE/DEAD assay. Data are presented as mean±S.D (n=3).

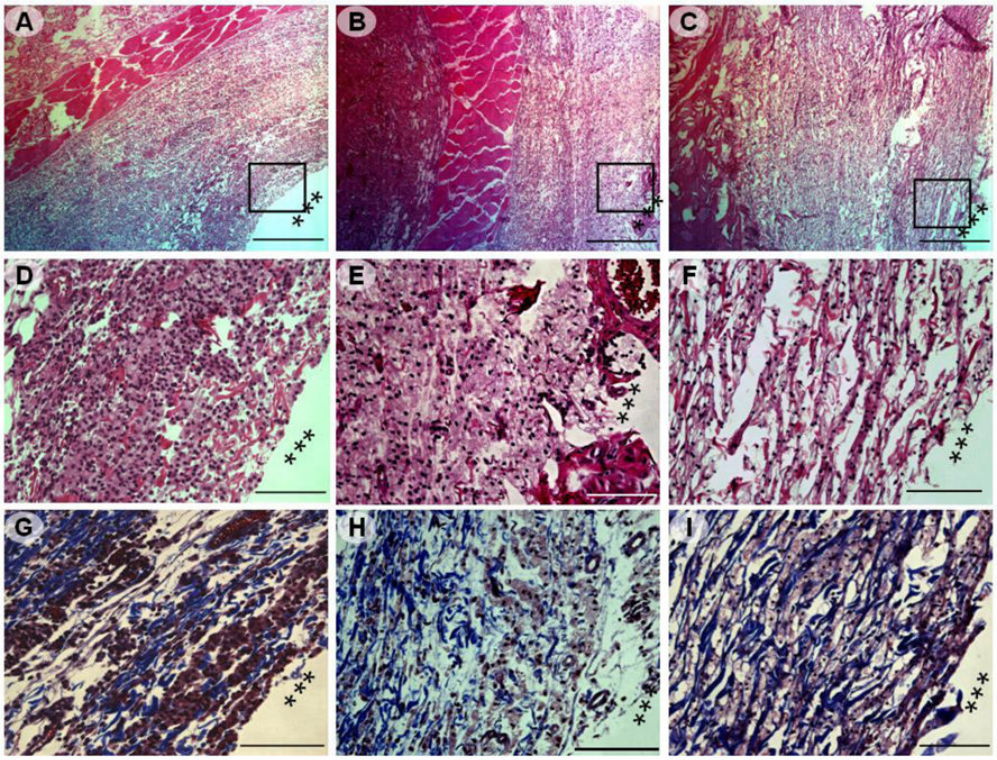

Fig. 7.

Photomicrographs of H&E and MTS stained sections of the tissues adjacent to ESHU injection site (marked by ***). The tissues were harvested after: 3 days (A, D, and G), 14 days (B, E, and H), and 28 days (C, F, and I). (A–C) Low magnification of images (40x, scale bar = 500 μm) of H&E stained tissue, rectangle frames indicated the field chosen for capture at higher magnifications. (D–F) H&E staining of the injection sites indicated a rapid decrease in inflammatory infiltrates over time. (200×, scale bar = 100 μm); (G–I) MTS staining of the injection site indicated collagen deposition (200×, scale bar = 100 μm).

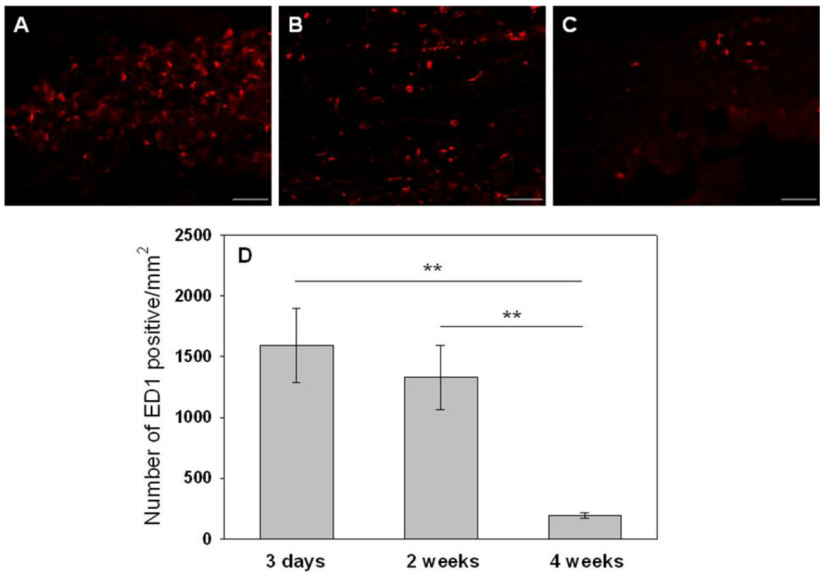

Fig. 8.

Representative photomicrographs (200×, scale bar = 60 μm) of injection sites immunohistochemically stained for ED1+ macrophages. Tissues were harvested after: (A) 3 days; (B) 14 days, and (C) 28 days. (D) The number of ED1+ macrophages decreased with time indicating a reduction in inflammatory response. Images from 5 random areas around the injection sites were used for quantification at each time point. Data represent mean±SD (n=5). ** $p<0.01$.

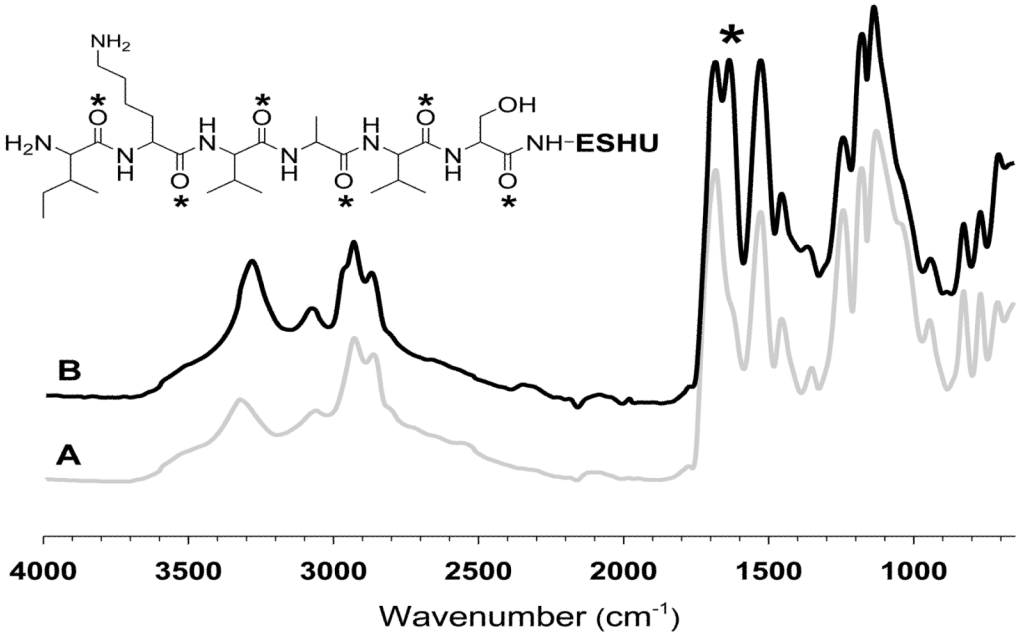

Fig. 9.

FTIR spectra of (A) NH_2-ESHU and (B) IKVAVS-ESHU. The carbonyl groups of the peptide bonds in IKVAVS-ESHU was observed at 1630 cm^{-1} (*) after IKVAVS incorporation.

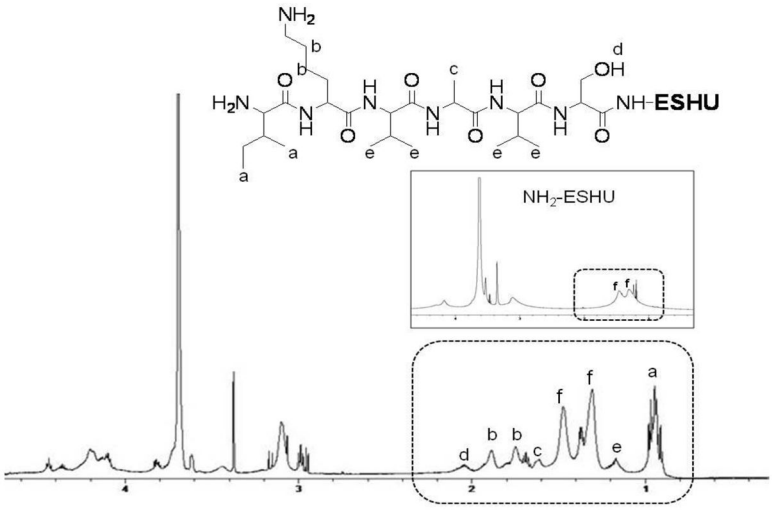

Fig. 10.

^{1}H FTNMR spectra of IKVAVS-ESHU in D_2O. The incorporation of IKVAVS was confirmed by appearance of new peaks between 0.8–2.2 ppm. The presence of **a**, **b**, **c**, **d**, and **e** protons indicates the presence of **Ile, Lys**, **Ala**, **Ser**, and **Val**, respectively. The methylene protons of ESHU backbone was marked as "**f**" (same as proton "**f**" in Fig 3).

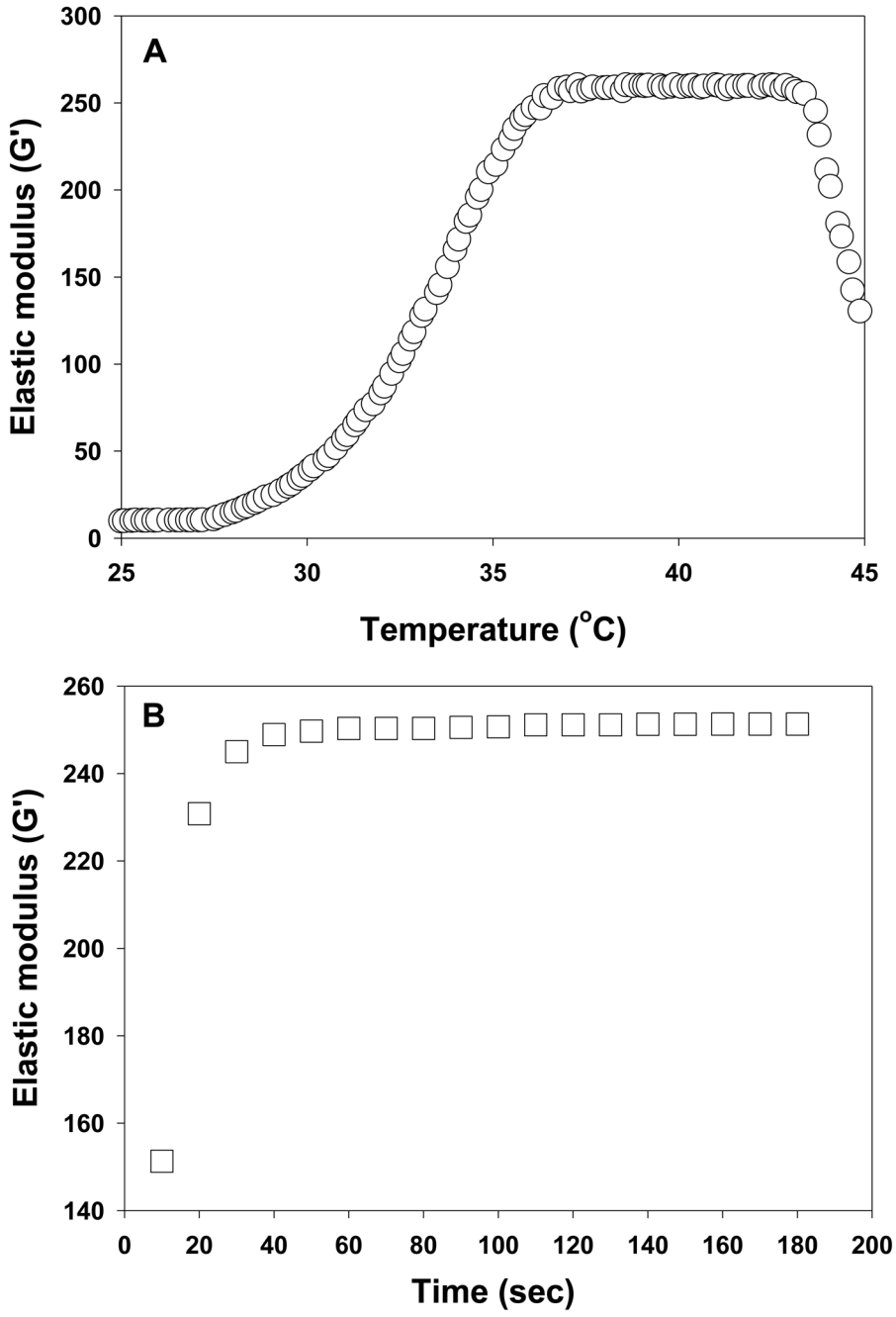

Fig. 11.

The elastic modulus of IKVAVS-ESHU. (A) Temperature sweep was recorded in the temperature range of 25–45°C (0.5°C/min) at concentrations of 15% (wt). The polymer solution showed rapid change of elastic modulus upon heating and gelled completely at 37°C. (B) Time sweep was recorded at 37°C at concentrations of 15% (wt) for 3min. The polymer solution became a gel in less than a minute.